E

Materials Science and Engineering C 32 (2012) 1571–1577

Contents lists available at SciVerse ScienceDirect

Materials Science and Engineering C

journal homepage: www.elsevier.com/locate/msec

Highly stable, protein capped gold nanoparticles as effective drug delivery vehicles for amino-glycosidic antibiotics

Lori Rastogi, Aruna Jyothi Kora, Arunachalam J. *

National Centre for Compositional Characterisation of Materials (NCCCM), Bhabha Atomic Research Centre, ECIL PO, Hyderabad – 500 062, India

ARTICLE INFO

Article history:
Received 25 November 2011
Received in revised form 26 February 2012
Accepted 22 April 2012
Available online 28 April 2012

Keywords:
Antibacterial
Antibiotics
Bovine serum albumin
Drug delivery
Gold nanoparticles
In vitro stability

ABSTRACT

A method for the production of highly stable gold nanoparticles (Au NP) was optimized using sodium borohydride as reducing agent and bovine serum albumin as capping agent. The synthesized nanoparticles were characterized using UV–visible spectroscopy, transmission electron microscopy, X-ray diffraction (XRD) and dynamic light scattering techniques. The formation of gold nanoparticles was confirmed from the appearance of pink colour and an absorption maximum at 532 nm. These protein capped nanoparticles exhibited excellent stability towards pH modification and electrolyte addition. The produced nanoparticles were found to be spherical in shape, nearly monodispersed and with an average particle size of 7.8 ± 1.7 nm. Crystalline nature of the nanoparticles in face centered cubic structure is confirmed from the selected-area electron diffraction and XRD patterns. The nanoparticles were functionalized with various amino-glycosidic antibiotics for utilizing them as drug delivery vehicles. Using Fourier transform infrared spectroscopy, the possible functional groups of antibiotics bound to the nanoparticle surface have been examined. These drug loaded nanoparticle solutions were tested for their antibacterial activity against Gram-negative and Gram-positive bacterial strains, by well diffusion assay. The antibiotic conjugated Au NP exhibited enhanced antibacterial activity, compared to pure antibiotic at the same concentration. Being protein capped and highly stable, these gold nanoparticles can act as effective carriers for drugs and might have considerable applications in the field of infection prevention and therapeutics.

1. Introduction

Gold nanoparticles are well-suited for a wide range of biological applications because of their unique physical and chemical properties [1]. The important advantages of gold nanoparticles are due to its (i) non-toxic and biologically inert nature [1–4]; (ii) convenient synthesis in a variety of sizes with great control [2]; (iii) effectual attachment of pharmaceutical compounds through electrostatic, covalent or non-covalent interactions [1,2]; and (iii) stabilizing agent tailorability for specific cell targeting, controlled release of the drug etc. [2]. Thus, gold nanoparticles were used as drug delivery vehicles for various antibiotics such as ciprofloxacin [5], streptomycin, gentamicin, neomycin, kanamycin, ampicillin, [6–8], vancomycin [9,10] and antileukemic drugs including doxorubicin hydrochloride [2] and 5- fluorouracil [11].

It is pertinent to note that in previous studies on Au NP conjugated with amino-glycosidic antibiotics, the conjugated products were a blue mixture of aggregates. For these aggregated conjugates, an increase in the antibacterial activity is reported based on well diffusion assay [7,8]. But, the diffusion of particle aggregates was questioned by other researchers and even with stable conjugates of Au NP-gentamicin no enhancement in antibacterial activity was observed [6]. The stability of nanoparticles over time (storage) and under different pH and electrolytic environments are the prerequisites for using nanoparticles for drug delivery applications [2]. Hence, in this study we have synthesized BSA capped gold nanoparticles and prepared stable conjugates of amino-glycosidic antibiotics including: streptomycin, neomycin, gentamicin and kanamycin. Then, these Au NP-antibiotic conjugates were tested against both the Gram classes of bacteria.

We have examined the use of bovine serum albumin (BSA) capped gold nanoparticles as carriers for the amino-glycosidic antibiotics. The interesting features of BSA motivated us to use this biopolymer as a model capping agent for gold nanoparticles. It is an abundant plasma carrier protein with well characterized structure [12,13]; and important physiological roles [12–14]. Moreover, protein capping makes the nanoparticles water dispersible and biocompatible at high electrolyte concentrations [15]. In addition, BSA as a stabilizing agent provides the necessary functional group for efficient loading of the drug on the nanoparticle surface [2]. Thus, the utilization of this protein capped gold nanoparticles with superior stability for drug delivery applications will be an added advantage.

The present study focuses on the synthesis, in *vitro* stability, characterization, functionalization of Au NP with amino-glycosidic class of antibiotics; and evaluation of their antibacterial activity on Gram-positive and Gram-negative bacteria.

* Corresponding author. Tel.: +91 40 27121365; fax: +91 40 27125463.
E-mail address: aruncccm@gmail.com (A. J.).

0928-4931/$ – see front matter © 2012 Elsevier B.V. All rights reserved.
doi:10.1016/j.msec.2012.04.044

2. Materials and methods

2.1. Materials

Chloroauric acid trihydrate (Sigma-Aldrich, Bengaluru, India), bovine serum albumin (BSA) fraction V (Sigma, Bengaluru, India) and sodium borohydride ($NaBH_4$) (E. Merck, Mumbai, India) were used for the synthesis. Amino-glycosidic antibiotics; streptomycin sulphate (Sigma, Bengaluru, India), neomycin sulphate, gentamicin sulphate and kanamycin sulphate (Himedia, Mumbai, India) were used to conjugate the generated gold nanoparticles. Millipore water was used as a solvent for all the experiments.

2.2. Synthesis of gold nanoparticles

To an aqueous solution of chloroauric acid containing 100 μg of Au^{3+}, a 100 μl of 10% BSA solution was added and stirred for 10 min. A 500 μl of an ice cold, freshly prepared solution of 0.1 M $NaBH_4$ was added slowly to the above reaction mixture, under continuous stirring. The synthesized nanoparticles have final gold and BSA concentrations of 0.125 mM and 0.05%, respectively in a volume of 20 ml, at pH 2.3. Control experiments indicated that the optimum particle size distribution and stability were achieved at the conditions mentioned above. The synthesized Au NP were washed by centrifuging (15,000 rpm, 30 min) and redispersing in MilliQ water in order to remove unreacted components. The washed preparation was then stored in an amber coloured bottle at room temperature. An aliquot of this preparation was used in all experiments. The effect of different variables such as concentrations of BSA and sodium borohydride; and stirring time etc. on nanoparticle synthesis has been studied (Supplementary Fig. 1).

2.3. Preparation of Au NP-antibiotic conjugates

A stock solution (10 mg/ml) of streptomycin sulphate, neomycin sulphate, gentamicin sulphate and kanamycin sulphate were prepared and stored at −20 °C. For the conjugation of gold nanoparticles with antibiotics, a 0.5 ml of the antibiotic stock was added drop wise to 5 ml of washed Au NP solution under stirring for 18 h condition. These Au NP-antibiotic conjugates were then stored at 4 °C and used for all further experiments.

2.4. Characterization of synthesized gold nanoparticles

The UV–visible absorption spectra of the prepared colloidal solutions were recorded using an Elico SL 196 spectrophotometer (Hyderabad, India), from 250 to 800 nm. The electrolyte stability of the synthesized nanoparticles was checked by adding 50 μl of different concentrations (0.025–0.1 M) of sodium chloride solutions to 1 ml of nanoparticles. The stability of the nanoparticle solutions was also studied in the pH window of 2.7–11. The size and shape of the nanoparticles were obtained with Philips CM200 (New York, USA) transmission electron microscope (TEM), operating at 200 kV. The samples were prepared by depositing a drop of colloidal solution on a carbon coated copper grid and drying at room temperature. The X-ray diffraction analysis was conducted with a Rigaku, Ultima IV diffractometer (Tokyo, Japan) using monochromatic Cu Kα radiation (λ = 1.5406 Å) running at 40 kV and 30 mA. The intensity data for the nanoparticle solution deposited on a glass slide was collected over a 2θ range of 35–70° with a scan rate of 1°/min. The IR spectra of the samples were recorded using a JASCO Inc., FT/IR-4200 spectrometer (Tokyo, Japan); over a spectral range of 1000–4000 cm^{-1}. The hydrodynamic diameter and zeta potential values of the functionalized nanoparticles were assessed with a Malvern Zetasizer Nanosystem (Worcestershire, UK).

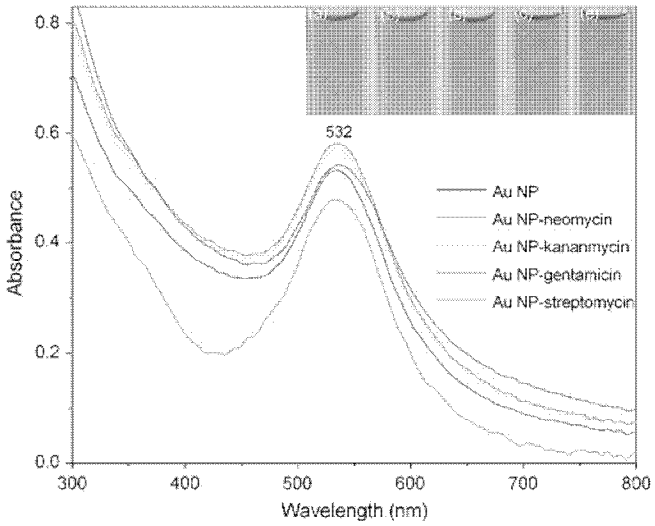

Fig. 1. The UV–visible absorption spectra of BSA capped gold nanoparticles loaded with amino-glycosidic antibiotics. The inset picture shows the colour of the solutions. (a) Au NP, (b) Au NP-streptomycin, (c) Au NP-neomycin, (d) Au NP-gentamicin and (e) Au NP-kanamycin.

2.5. Antibacterial assay

These drug loaded nanoparticle solutions were tested for their antibacterial activity against Gram-negative (*Escherichia coli* ATCC

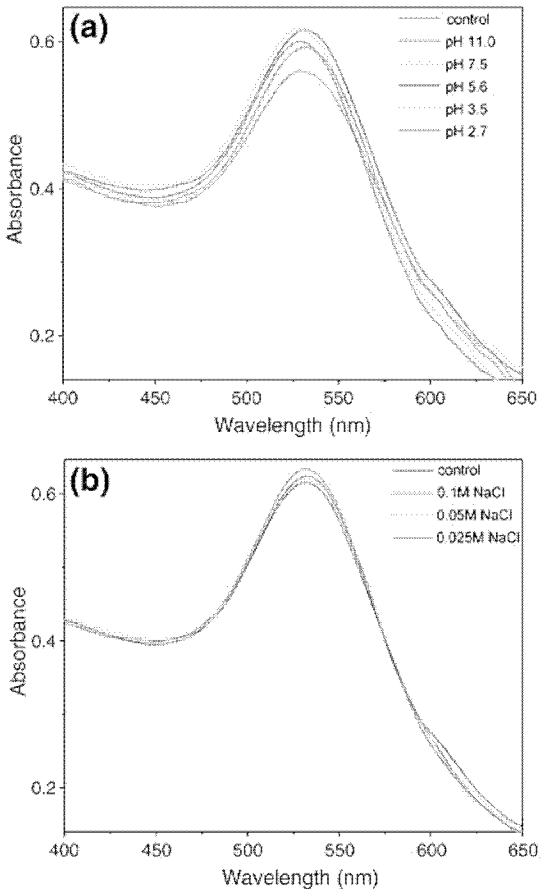

Fig. 2. The UV–vis absorption spectra showing the *in vitro* stability of protein stabilized gold nanoparticles, at (a) pH window of 2.7–11 and (b) sodium chloride concentrations of 0.025–0.1 M.

25922, *Pseudomonas aeruginosa* ATCC 27853) and Gram-positive (*Staphylococcus aureus* ATCC 25923) bacterial strains, using well diffusion assay. All the glassware, plasticware and media used were sterilized in an autoclave at 121 °C for 20 min. The bacterial suspension was prepared by growing a single colony overnight in nutrient broth and then adjusting the turbidity to 0.5 McFarland standard. Mueller Hinton agar plates were inoculated with this bacterial suspension and 10 μl of solution containing 0.25 μg of nanoparticles conjugated with 10 μg of antibiotics was added to the center well with a diameter of 6 mm. Negative and positive control wells were maintained with 0.25 μg of nanoparticles and 10 μg of antibiotics, respectively. These plates were incubated at 37 °C for 24 h in a bacteriological incubator and the zone of inhibition (ZOI) was measured by subtracting the well diameter from the total inhibition zone diameter. Three independent experiments were carried out with each bacterial strain.

3. Results and discussion

3.1. UV–visible spectroscopy (UV–vis)

The synthesis of nanoparticles was recorded by measuring the absorption spectra of synthesized gold nanoparticles. The formation of gold nanoparticles was confirmed from the appearance of pink colour in the reaction mixture and an absorption maximum at 532 nm (Fig. 1). The UV–vis spectra of the nanoparticles conjugated with various antibiotics were also measured. It has been observed that the peak position and solution color does not change even after conjugating with antibiotics, indicating the non-aggregated nature of the functionalized nanoparticles (Fig. 1).

3.2. Stability of synthesized gold nanoparticles

The solutions of gold nanoparticles capped with BSA are clear pink, without any colour change and visual aggregation, even after one year of storage at room temperature. This observation is also validated from the absorbance spectra of nanoparticles, which showed hardly any change in the λ_{max} and intensity values with storage time (Supplementary Fig. 2). In addition, the stability of the nanoparticles is unaffected by the pH changes and high salt concentration (Fig. 2). These solutions are stable in both acidic and alkaline media, from a pH range of 2.7–11, with no obvious change in absorbance intensity and peak position at 532 nm. And, even the addition of sodium chloride up to 0.1 M did not cause any particle aggregation, indicating superior electrolyte stability. Thus, the gold nanoparticles formed by this method are highly stable and well dispersed in nature. A similar feature of in vitro stability was reported for gold nanoparticles stabilized with gellan gum [2], tea phytochemicals [4] and guavanoic acid [16].

3.3. Transmission electron microscopy

Fig. 3 shows the TEM images of the gold nanoparticles capped with 0.05% BSA. The synthesized nanoparticles are spherical in shape, nearly monodispersed and with an average particle size of 7.8 ± 1.7 nm. The electron micrographs of the Au NP-streptomycin are depicted in Fig. 4. These nanoparticles retained the spherical morphology and the average particle size obtained from the corresponding diameter distribution was about 8.6 ± 2.8 nm (Fig. 4d). This data supports the absence of nanoparticle aggregation after conjugation, which is substantiated from the absorption spectra and solution colour (Fig. 1). The selected-

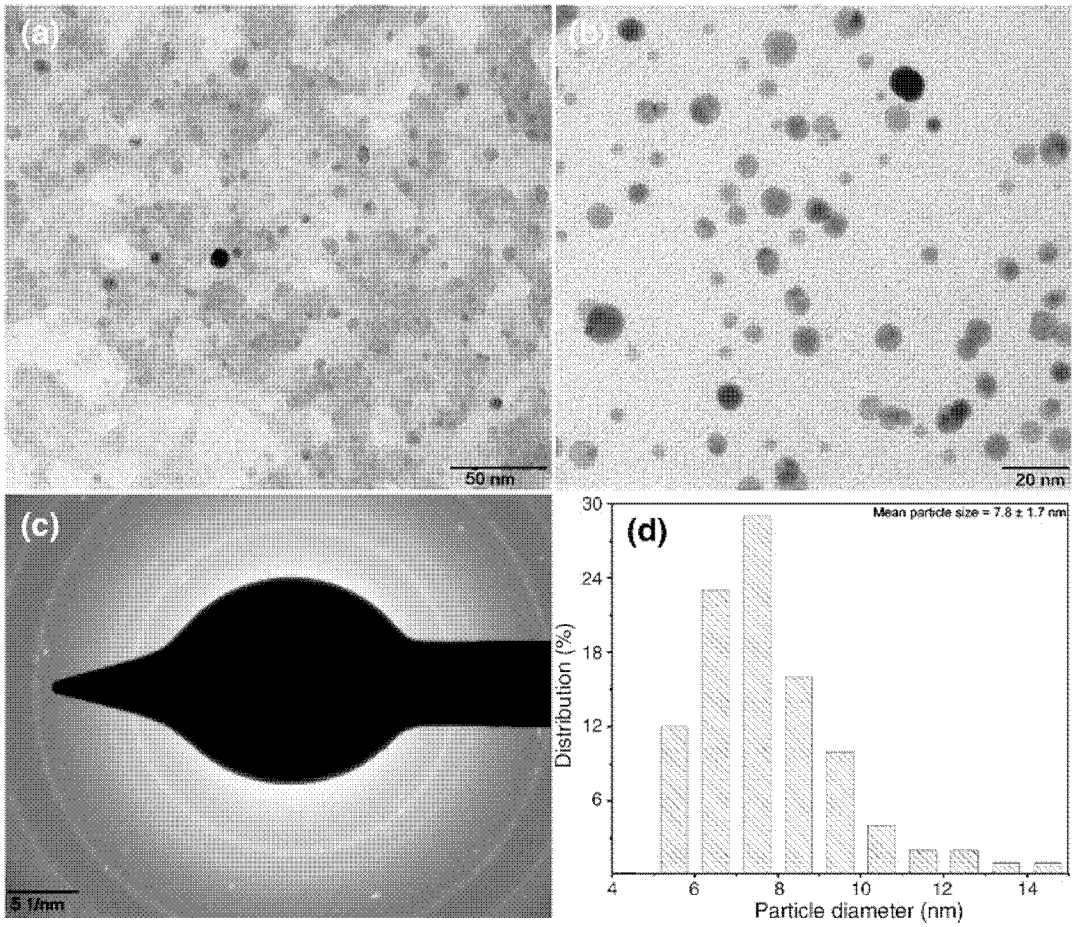

Fig. 3. TEM images of produced gold nanoparticles, at (a) 50 nm and (b) 20 nm scale. (c) corresponding SAED pattern and (d) histogram showing the particle size distribution.

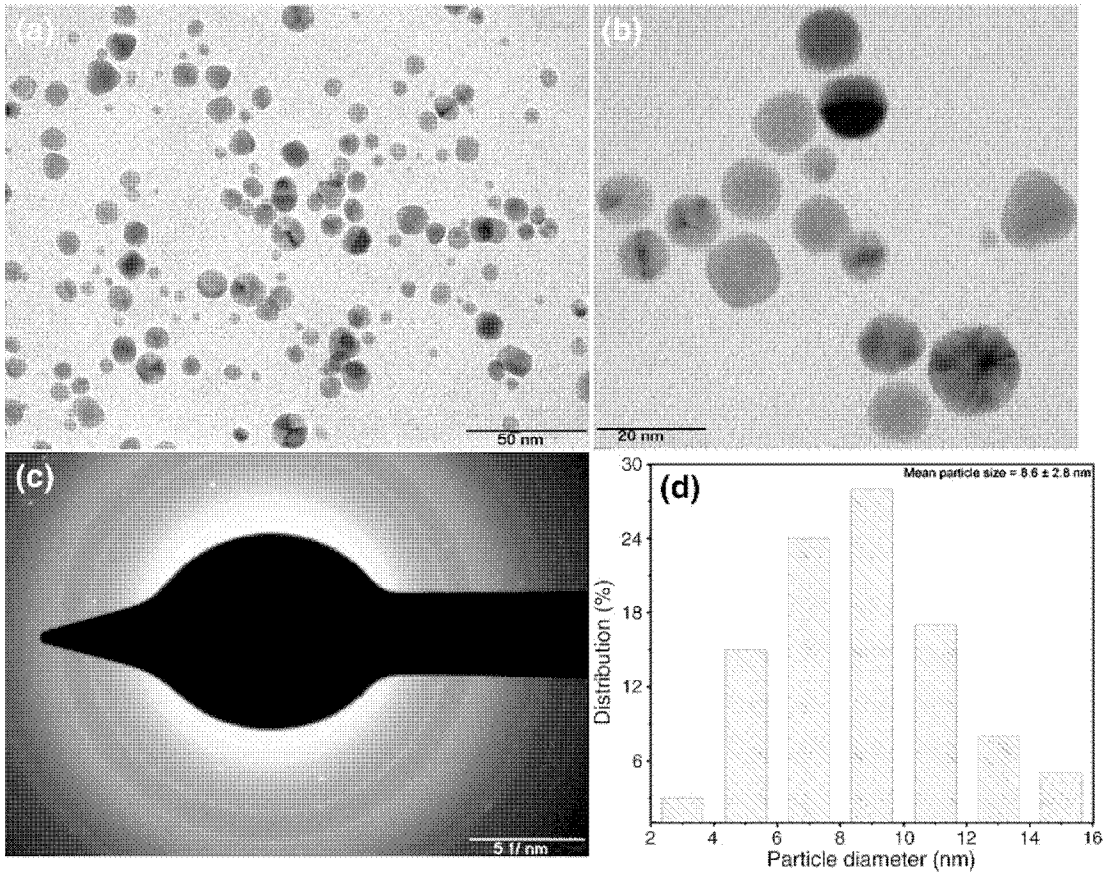

Fig. 4. TEM images of Au NP-streptomycin, at (a) 50 nm and (b) 20 nm scale. (c) corresponding SAED pattern and (d) histogram showing the particle size distribution.

area electron diffraction (SAED) patterns depicted in Figs. 3 and 4 exhibit concentric rings, indicate that these nanoparticles are highly crystalline. These rings can be attributed to the diffraction from the (111), (200), (220) and (311) planes of face centered cubic (fcc) gold. The effect of antibiotic loading on the hydrodynamic diameter of nanoparticles was also investigated (Table 1). The data establishes that the functionalization of nanoparticles with antibiotics may not cause much change in the hydrodynamic radius, thereby revealing the non-aggregated nature of drug loaded nanoparticles.

3.4. X-ray diffraction (XRD)

The XRD technique was used to determine and confirm the crystal structure of prepared gold nanoparticles. There were three well-defined characteristic diffraction peaks at 38.0°, 44.9° and 64.5°, respectively, corresponding to (111), (200) and (220) planes of face centered cubic (fcc) crystal structure of metallic gold (Fig. 5). The interplanar spacing values ($d_{h\ k\ l}$) values (2.366, 2.017 and 1.443 Å) calculated from the XRD spectrum of gold nanoparticles are in agreement with the standard gold values. Thus, the XRD pattern further corroborates the highly crystalline nature of nanoparticles observed from SAED patterns (Figs. 3 and 4). The lattice constant calculated from this pattern was 4.071 Å, a value which is in agreement with the value reported in literature for gold (JCPDS PDF card 04-0784). Also, the broadening of the diffraction peaks was observed owing to the effect of nano-sized particles.

Table 1
The hydrodynamic diameter and zeta potential values of the functionalized gold nanoparticles.

Nanoparticles	Size (nm)	Zeta potential (mV)
Au NP	55.44	+11.3
Au NP-streptomycin	42.45	+16.3
Au NP-kanamycin	52.58	+12.6
Au NP-gentamicin	63.96	+12.3
Au NP-neomycin	72.76	+11.7

3.5. Fourier transform infrared spectroscopy (FTIR)

The nature of binding of antibiotics to the nanoparticles has been investigated by FTIR technique (Fig. 6). All the amino-glycosidic

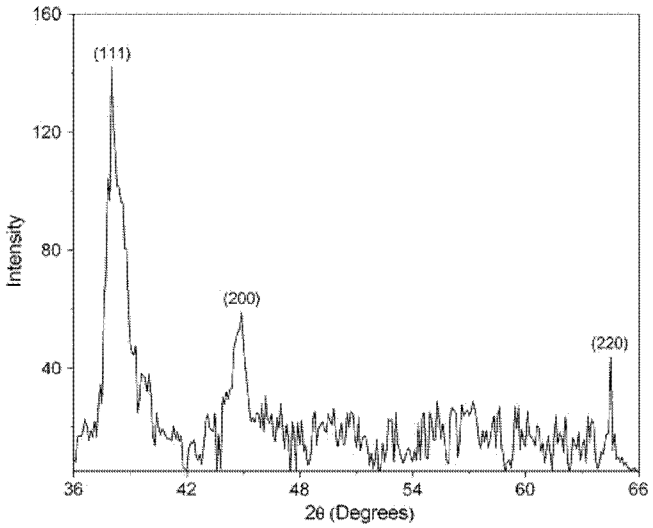

Fig. 5. The X-ray diffraction pattern of synthesized gold nanoparticles, indicating face centered cubic (fcc) crystal structure.

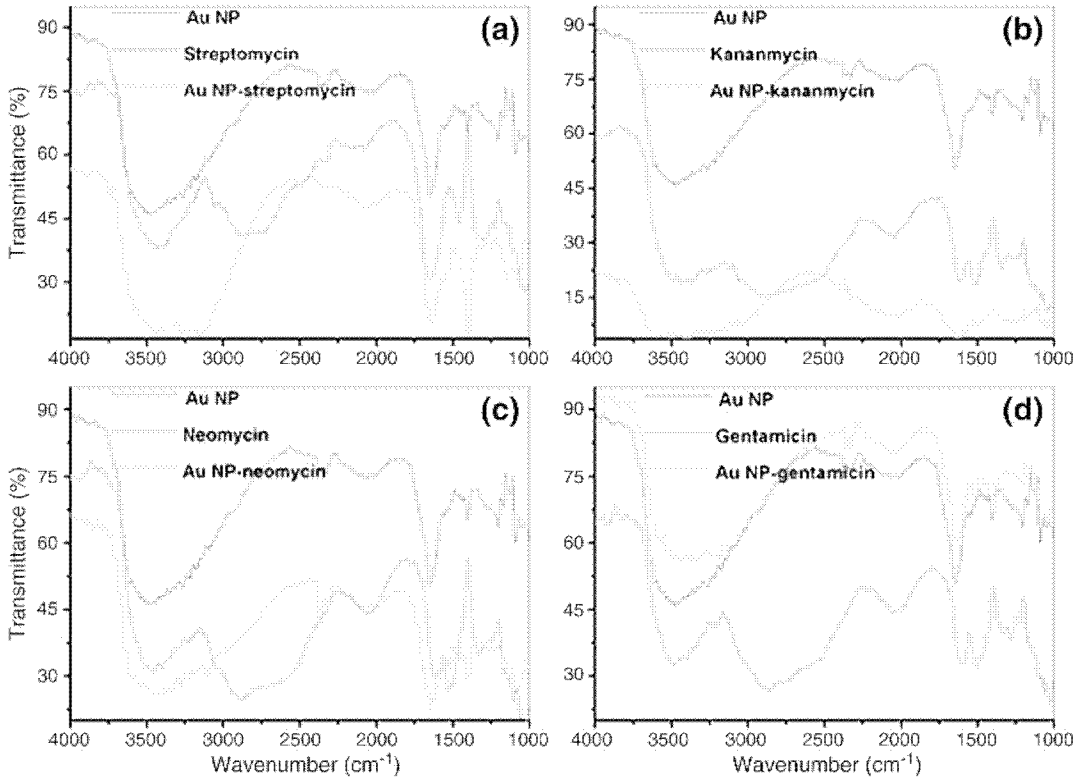

Fig. 6. FTIR spectra of (a) Au NP, streptomycin and Au NP-streptomycin, (b) Au NP, kanamycin and Au NP-kanamycin, (c) Au NP, neomycin and Au NP-neomycin and (d) Au NP, gentamicin and Au NP-gentamicin.

antibiotics revealed characteristic absorption bands corresponding to N–H bending frequency at 1600–1652 cm^{-1}. The distinctive NH_2 stretching frequencies of the amine groups were noticed at 3435, 3491, 3456 and 3482 cm^{-1} for the antibiotics streptomycin, kanamycin, neomycin and gentamicin, respectively. In the case of antibiotic conjugated gold nanoparticles, the corresponding NH_2 peaks were broadened and shifted to higher wavelengths. Based on the data, it can be concluded that amino groups of the antibiotics are bound to gold nanoparticle surface. In a study carried out with amino-glycosidic antibiotics protected gold nanoparticles, similar observations were noted [7]. It is reported that the nitrogen atom of the NH moiety of piperazine group binds on the gold surface, in the case of ciprofloxacin protected gold nanoparticles [5]. From the data, it is demonstrated that the capped gold nanoparticles act as effective anchor for transporting large amount of antibiotics on their surface via electrostatic interaction between the amine group of drugs and gold nanoparticles [7,9,13]. The absorption peak at 1399 cm^{-1} was observed only for gold nanoparticles, attributed to symmetrical stretching vibration of carboxylate group. The exhibited peak at 1600–1652 cm^{-1} for gold nanoparticles can also be identified as amide I, which arises due to the carbonyl stretching vibrations in the amide linkages of the proteins. Further, these IR data also confirms the coating of the nanoparticles by the protein BSA.

3.6. Antibacterial activity

The highly stable nanoparticles were used to load the amino-glycosidic antibiotics (streptomycin, neomycin, gentamicin and kanamycin). After 24 h of incubation at 37 °C, the negative control plates loaded with 0.25 μg of BSA capped nanoparticles did not produce any ZOI. These nanoparticles did not produce any ZOI even at 5 μg loading (Supplementary Fig. 3). While, growth suppression was observed in plates loaded with antibiotics and Au NP-antibiotics. The antibiotic functionalized nanoparticles showed superior antibacterial activity, compared to pure antibiotic at the same concentration of 10 μg. The % enhancement in antibacterial activity for Gram-negative *E. coli* and *P. aeruginosa* strains was in the order of Au NP-streptomycin > Au NP-neomycin > Au NP-gentamicin > Au NP-kanamycin (Figs. 7 and 8). In the case of Gram-positive *S. aureus* strain, the order was found to be Au NP-streptomycin > Au NP-kanamycin > Au NP-neomycin > Au NP-gentamicin (Fig. 9). Among these amino-glycosidic antibiotics, streptomycin loaded nanoparticles has shown highest activity against both the Gram classes of bacteria. This probably depends upon the zeta potential values of the nanoparticle solutions (Table 1). The zeta

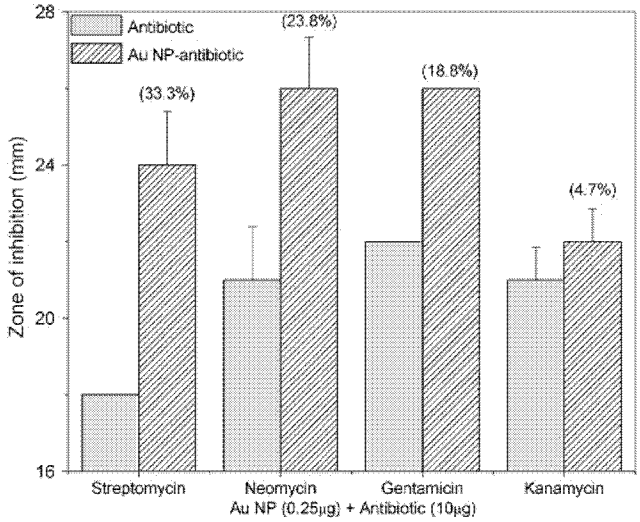

Fig. 7. Inhibition zones observed for the strain *E. coli* ATCC 25922 with antibiotic and antibiotic functionalized gold nanoparticles. Error bars represent standard deviation of the mean. Values given in ( ) indicate the % enhancement in antibacterial activity.

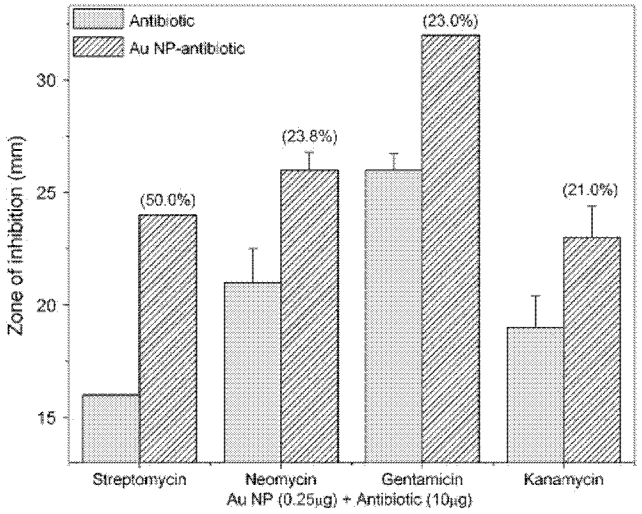

Fig. 8. Inhibition zones observed for the strain *P. aeruginosa* ATCC 27853 with antibiotic and antibiotic functionalized gold nanoparticles. Error bars represent standard deviation of the mean. Values given in () indicate the % enhancement in antibacterial activity.

potential value of Au NP-streptomycin is +16.3, which is highest compared to other preparations. Such a positive correlation between antibacterial activity and zeta potential of the nanoparticles was previously reported for chitosan tripolyphosphate nanoparticles loaded with metal ions [17]. Under acidic environment, protonation of amino groups of antibiotics results in positive charge on the surface of nanoparticles. Thus, the positively charged functionalized nanoparticles bind to the negatively charged bacterial cell surface and disrupt the cellular functioning [17–19]. Also, the zeta potential imparts stability to the aqueous nanoparticle solutions, which is necessary for exhibiting any biological activity. When compared with Gram-negative bacteria, Gram-positive strain *S. aureus* is more susceptible to functionalized nanoparticles except Au NP-gentamicin, which possibly depends upon cell wall structure [19].

Such an enhancement in antimicrobial activity was observed for drugs conjugated to gold nanoparticles including; streptomycin, gentamicin, neomycin, ampicillin, kanamycin, vancomycin [7–10] and 5-fluorouracil [11]. To further assess our results, we have compared our values with the available report using corresponding bacterial strains,

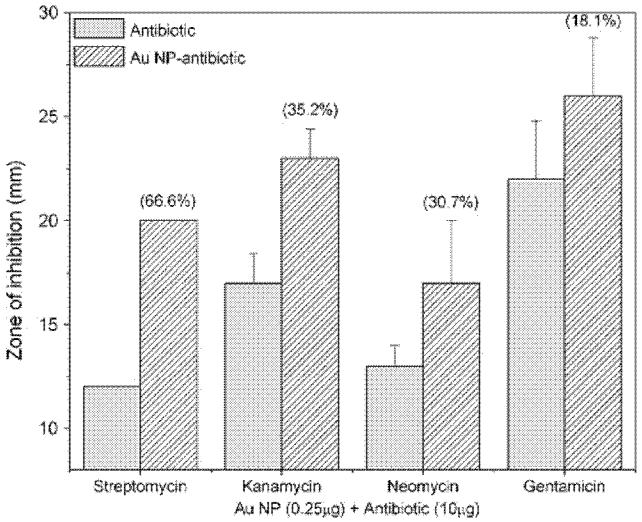

Fig. 9. Inhibition zones observed for the strain *S. aureus* ATCC 25923 with antibiotic and antibiotic functionalized gold nanoparticles. Error bars represent standard deviation of the mean. Values given in () indicate the % enhancement in antibacterial activity.

at equivalent concentrations. For *E. coli* the % enhancement in activity was found to be higher by 2.7 and 3.6 times, for Au NP-streptomycin and Au NP-neomycin, respectively. In the case of *P. aeruginosa*, it was more by a factor of 2.1 and 1.4 for the respective Au NP-streptomycin and Au NP-gentamicin. While for *S. aureus*, the activity was superior by 2.1 and 1.7 times for the corresponding Au NP-streptomycin and Au NP-gentamicin [7]. Thus, the antibacterial activity of drug loaded gold nanoparticles observed by us is greater than the reported values. Similarly increased cytotoxic effects on human glioma cell lines were demonstrated with gold nanoparticles loaded with doxorubicin hydrochloride, an anticancer antibiotic [2]. It was also established that the gold nanoparticles conjugated with antibiotics (ampicillin, streptomycin and kanamycin) exhibit greater thermal stability as compared to corresponding free antibiotics [8]. When gold nanoparticles were used as carriers, the release of drug for an extended period of time was observed for ciprofloxacin [5]. In addition, the capped proteins retain their secondary structure on nanoparticle surface and protein capping makes the nanoparticles biocompatible [15]. It is reported that the functional unit used as a capping/stabilizing agent plays an important role and determines the tissue distribution profile of gold nanoparticles. In experiments carried out with swine, the majority of the dosed gold was located in the liver for the gum arabic-stabilized Au NP, while it was present in the lungs for the maltose stabilized Au NP [3]. Earlier studies carried out with BSA capped gold nanoparticles have shown the dependence of cellular uptake both on the size and surface coating of the nanoparticles [20]. Thus, our results suggest that these stable gold nanoparticles can act as efficient drug delivery vehicles and might have considerable biomedical applications like detection and therapy of various diseases after conjugation with suitable therapeutic molecules. The possible reasons for enhancement of antibacterial activity of antibiotic loaded gold nanoparticles are the superior stability with no shift in the UV–vis spectrum and solution colour; and transport of a large number of antibiotic molecules into a highly localized volume at the site of (in the proximity of) bacterium-particle contact [1,6].

4. Conclusions

In this study, a method for the production of highly stable, protein capped gold nanoparticles is reported. The generated nanoparticles showed excellent *in vitro* stability towards pH changes and high salt concentration, which are necessary for biomedical applications. The nanoparticles were functionalized with various amino-glycosidic antibiotics and evaluated against Gram-negative and Gram-positive bacteria. The conjugated nanoparticles exhibited enhanced antibacterial activity, compared to pure antibiotic. The results suggest that these metal nanoparticles can be used as effective carriers for antibiotic molecules and have potential biosensing [15] and cell targeting [3,20] applications.

Supplementary data related to this article can be found online at http://dx.doi.org/10.1016/j.msec.2012.04.044.

Acknowledgements

We thank Dr. S.V. Narasimhan, Associate Director and Dr. Tulsi Mukherjee, Director, Chemistry Group, BARC for their constant support and encouragement. The support rendered for TEM measurements by the Sophisticated Analytical Instrument Facility (SAIF) at IIT-Bombay, Mumbai is gratefully acknowledged.

References

[1] D. Pissuwan, T. Niidome, M.B. Cortie, J. Control. Release 149 (2011) 65–71.
[2] S. Dhar, E.M. Reddy, A. Shiras, V. Pokharkar, B.L.V. Prasad, Chem. Eur. J. 14 (2008) 10244–10250.
[3] M.F. Genevieve, W.C. Stan, K. Dae Young, K. Raghuraman, K. Kavita, C. Nripen, K. Kattesh, Nanomed. Nanotechnol. Biol. Med. 5 (2009) 128–135.

[4] S.K. Nune, N. Chanda, R. Shukla, K. Katti, R.R. Kulkarni, S. Thilakavathy, S. Mekapothula, R. Kannan, K.V. Katti, J. Mater. Chem. 19 (2009) 2912–2920.
[5] R.T. Tom, V. Suryanarayanan, P.G. Reddy, S. Baskaran, T. Pradeep, Langmuir 20 (2004) 1909–1914.
[6] G. Burygin, B. Khlebtsov, A. Shantrokha, L. Dykman, V. Bogatyrev, N. Khlebtsov, Nanoscale Res. Lett. 4 (2009) 794–801.
[7] A. Nirmala Grace, K. Pandian, Colloids Surf., A 297 (2007) 63–70.
[8] B. Saha, J. Bhattacharya, A. Mukherjee, A. Ghosh, C. Santra, A. Dasgupta, P. Karmakar, Nanoscale Res. Lett. 2 (2007) 614–622.
[9] H. Gu, P.L. Ho, E. Tong, L. Wang, B. Xu, Nano Lett. 3 (2003) 1261–1263.
[10] A. Mohammed Fayaz, M. Girilal, S.A. Mahdy, S.S. Somsundar, R. Venkatesan, P.T. Kalaichelvan, Process Biochem. 46 (2011) 636–641.
[11] V. Selvaraj, M. Alagar, Int. J. Pharm. 337 (2007) 275–281.
[12] M. Iosin, F. Toderas, P.L. Baldeck, S. Astilean, J. Mol. Struct. 924–926 (2009) 196–200.
[13] N.S. Jha, N. Kishore, Thermochim. Acta 482 (2009) 21–29.
[14] S. Pramanik, P. Banerjee, A. Sarkar, S.C. Bhattacharya, J. Lumin. 128 (2008) 1969–1974.
[15] P. Murawala, S.M. Phadnis, R.R. Bhonde, B.L.V. Prasad, Colloids Surf., B 73 (2009) 224–228.
[16] S. Khaleel Basha, K. Govindaraju, R. Manikandan, J.S. Ahn, E.Y. Bae, G. Singaravelu, Colloids Surf., B 75 (2010) 405–409.
[17] W.-L. Du, S.-S. Niu, Y.-L. Xu, Z.-R. Xu, C.-L. Fan, Carbohydr. Polym. 75 (2009) 385–389.
[18] L. Qi, Z. Xu, X. Jiang, C. Hu, X. Zou, Carbohydr. Res. 339 (2004) 2693–2700.
[19] S. Inphonlek, N. Pimpha, P. Sunintaboon, Colloids Surf., B 77 (2010) 219–226.
[20] D.B. Chithrani, M. Dunne, J. Stewart, C. Allen, D.A. Jaffray, Nanomed. Nanotechnol. Biol. Med. 5 (2009) 118–127.